Chapter 1

A Double *In Vivo* Biotinylation Technique to Assess Erythrocyte Turnover in Blood Circulation

Sreoshi Chatterjee and Rajiv K. Saxena

Additional information is available at the end of the chapter

http://dx.doi.org/10.5772/intechopen.69133

Abstract

We have developed a new double *in vivo* biotinylation (DIB) technique that may be used for assessing turnover patterns of erythrocytes in circulation. This technique involves two successive *in vivo* biotinylation steps, interspersed by a period of 5–30 days, which would enable us to tag with biotin a population of erythrocytes entering blood circulation over a defined period of time, between the two biotinylation steps. As such we can track the age-related changes in a lifetime of the circulating erythrocytes, or we can simultaneously study two defined age cohorts of aged as well as young erythrocytes in circulation. We have extensively used this technique to look at erythrocyte loss in mouse models of anemia induced by (a) heavy metal cadmium (Cd), (b) herbicide Paraquat (PQ), (c) carbon nanotubes (CNTs), and (d) autoantibody in autoimmune hemolytic anemia (AIHA). We have found that the pattern of erythrocyte removal is distinctly different in different models of murine anemia. In certain types of anemia (CNT and AIHA), younger erythrocytes in blood circulation are preferentially removed, whereas in other cases (Cd and PQ), old erythrocytes are specifically eliminated.

Keywords: DIB technique, flow cytometry, erythrocyte turnover, anemia, mouse models of anemia, cadmium, Paraquat, carbon nanotubes, autoantibody, AIHA

1. Introduction

Erythrocytes constitute almost 99.9% of all blood cells, excluding platelets. Erythrocytes have a definite lifespan in the circulation during which time they shuttle through the entire body several times exchanging respiratory gases between tissues and organs. The lifespan of human and murine erythrocytes has been estimated to be around 120 and 50 days, respectively, indicating

that roughly 1% of all circulating erythrocytes in human and 2% in mice are destroyed each day [1–3]. Erythrocytes undergo repetitive cycles of oxidation and reduction during gaseous exchange, are regularly exposed to severe osmotic shock while passing through the kidney medulla, and have to squeeze through very narrow blood capillaries. As the erythrocytes age in circulation, these repeated insults result in accumulation of several changes in the cell, particularly in the membrane composition. These damaged erythrocytes are prone to destruction in the reticuloendothelial system (RES) in the spleen, bone marrow, and liver [4].

Studies in the past have aimed to decipher the actual kinetics of erythrocyte turnover in circulation, but their approaches have been marred by the unavailability of a suitable technique to identify erythrocytes of different age groups. Mostly they have relied upon buoyant density of the erythrocytes [5, 6] or hyper-transfusion studies [7]. Later with the advent of biotinylation studies [8–10], things became clearer, and finally with the novel double *in vivo* biotinylation (DIB) technique developed in our lab [11, 12], we have now been able to solve the mystery of the kinetics of erythrocyte survival in the blood [11–16]. Studies on erythrocyte survival kinetics and the associated age-related changes in buoyant density, autofluorescence, and phosphatidylserine (PS) externalization have extensively been reviewed in Saxena et al. [16].

Using the DIB technique, erythrocyte turnover kinetics in a normal murine system is now well understood. However in the case of anemia, where the homeostasis between erythrocyte destruction and erythropoiesis is disturbed, the erythrocyte turnover pattern may completely alter. To understand the fate of erythrocyte turnover in conditions of anemia, we studied four mouse models of experimental anemia, namely anemia induced by (a) toxic heavy metal cadmium (Cd) ions [17], (b) herbicide Paraquat (PQ) [18], (c) carbon nanotubes (CNTs) [19], and (d) autoantibody in autoimmune hemolytic anemia (AIHA) [20].

2. The double *in vivo* biotinylation (DIB) technique

Advent of the DIB technique, recently developed in our laboratory, has made it possible to simultaneously enumerate and study erythrocytes of different age groups in blood circulation [11, 12, 16]. In the DIB protocol, circulating erythrocytes were biotinylated in two steps by intravenous administration of biotin-X-N-hydroxysuccinimide ester (BXN), through the tail vein of mice. The first step of high-intensity biotinylation involved three daily intravenous (*i.v.*) injections of biotin (1 mg), followed after few days by a low-intensity biotin injection with a single lower dose (0.6 mg). The first step labels all the erythrocytes present in circulation at the time of injection, while the second step labels the fresh erythrocytes that were released in circulation in the period between the two biotinylation steps. At any time point after the second biotinylation, biotin intensity on circulating erythrocytes could be analyzed by flow cytometry after staining the erythrocytes with streptavidin coupled to an appropriate fluorochrome [11, 12, 16]. As such erythrocytes in circulation could be grouped into three distinct cohorts: (i) biotin^{negative} erythrocytes that represents the fresh erythrocytes that were released in the blood after the second step of biotinylation, (ii) biotin^{low} erythrocytes

that consists of the cohort of erythrocytes released in the blood between the two steps of biotinylation, and (iii) biotin^{high} erythrocytes that comprise the residual erythrocytes from the ones that were present in circulation at the time of the first biotinylation step [16]. The DIB protocol has been summarized in **Figure 1**.

Time interval between the two biotin injections can be altered according to the requirement of the experiment [16]. In DIB protocol A, a window of 5 days is provided between the two steps. This enables us to track the circulating erythrocytes from the moment of its release into the bloodstream till the end of its lifespan. Alternatively by introducing a long gap (of about 30 days) in DIB protocol B, two defined cohorts of aged as well as young erythrocytes in circulation can be identified and studied simultaneously. For details, see **Figure 1**.

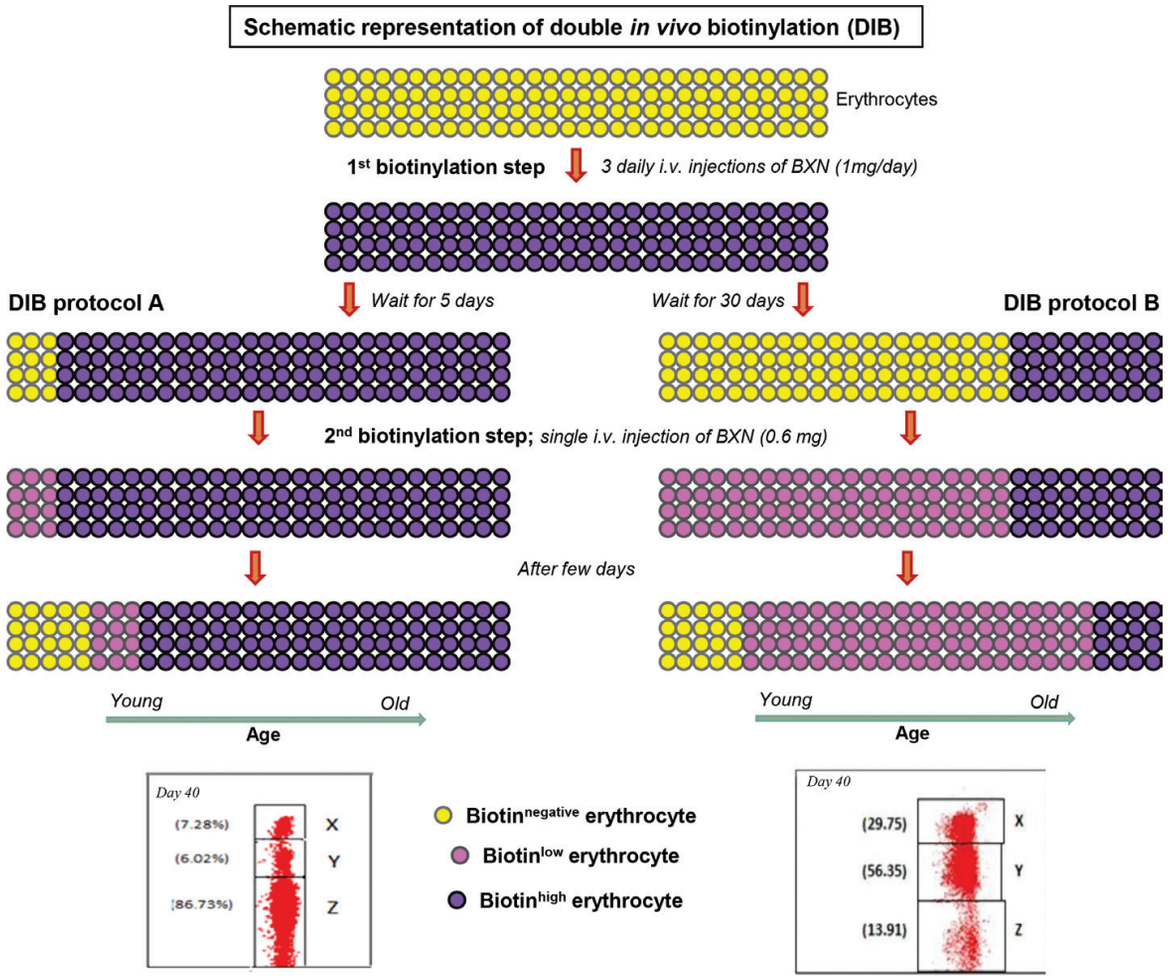

Figure 1. Double *in vivo* biotinylation (DIB) technique. C57BL/6 mice were given three daily *i.v.* doses of 1 mg BXN (first biotinylation step), followed, after a rest for several days, by a single additional dose of 0.6 mg BXN (second biotinylation step). Biotin label on erythrocytes was examined at different time points by bleeding the mice and staining the cells with streptavidin-APC followed by flow cytometry. In DIB protocol A, a window of 5 days is provided between the two biotinylation steps; in DIB protocol B, a long gap of 30 days is introduced. Principle of the technique and the residual biotin label on circulating erythrocytes are shown above. Erythrocyte populations in boxes X, Y, and Z represent biotin^{high}, biotin^{low}, and biotin^{negative} erythrocytes, respectively; values in parentheses represent percentage of cells in different boxes.

3. Erythrocyte turnover in the blood

Erythrocytes have a definite lifespan in the circulation during which time they shuttle through the entire body several times exchanging respiratory gases between tissues and organs. Using the DIB technique, we have been able to follow the survival kinetics of a cohort of erythrocytes of defined age, with a degree of precision not possible so far. Based on this technique, Khandelwal and Saxena [11] described the triphasic nature of survival kinetics of blood erythrocytes in circulation. This profile has been depicted in **Figure 2**. In this system, a defined cohort of erythrocytes remained more or less constant till 10 days after their release in circulation and

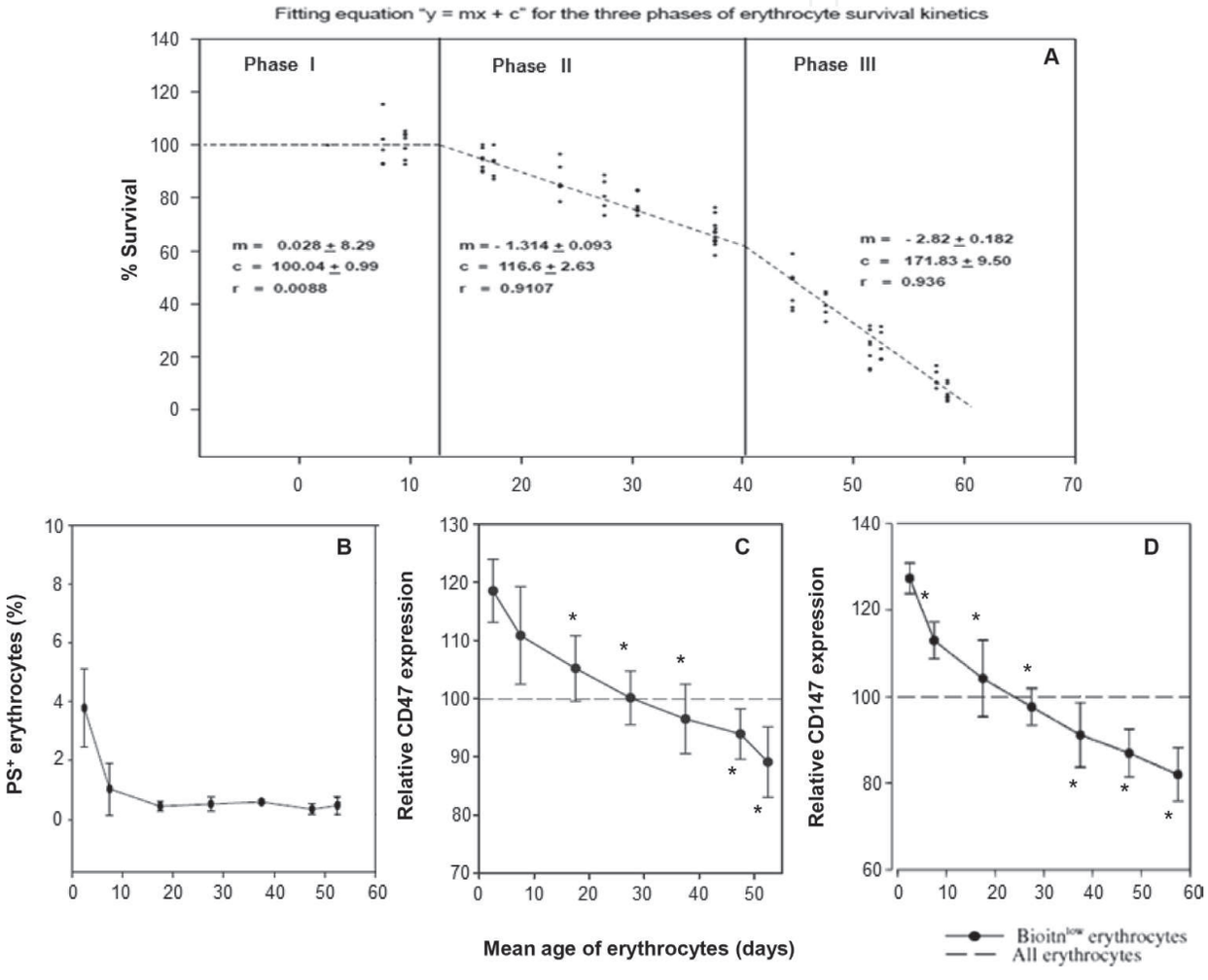

Figure 2. Survival kinetics of erythrocytes in circulation. C57BL/6 mice were DIB labeled following protocol A. At different time points, the biotin^{low} population was assessed as percentage of all circulating erythrocytes and followed throughout their lifespan in the blood. Panel A shows the survival kinetics of murine erythrocytes. Correlation coefficients and slopes of the three phases of the decay curve have been calculated (n = 14). PS externalization and expression of CD47 and CD147 were studied on the biotin^{low} population during its lifespan in the blood. Panel B shows the proportion of PS$^+$ erythrocytes. As compared to the first time point, the decline in PS expression on all subsequent time points was statistically significant. CD47 and CD147 expression are given in panels C and D, respectively. Mean CD47 and CD147 expression on the biotin^{low} population has been expressed as percentage of the mean expression on all blood erythrocytes. Each point in the graph represents mean ± SD of observations. n = 5. *$p < 0.05$ for comparison of the groups. Statistical analysis was done using Student t-test.

started to decline constantly thereafter, indicating a random destruction irrespective of age. The rate of this decline increased after about 40 days in circulation, suggesting the onset of an age-dependent selective killing of erythrocytes [11, 15]. Thus the true picture of erythrocyte destruction in mice circulation appears to be a combination of both random killing, at least in the first segment of the life cycle, and the age-dependent destruction, especially in the latter part of the life span.

The factors that drive such unique survival kinetics of circulating erythrocytes are not clearly understood. The role of PS externalization might be critical in this respect. Annexin V staining of biotin^{low} erythrocytes at different time points reveals that PS extrusion is more efficient in younger erythrocytes rather than in senescent ones (**Figure 2B**) [12]. It is likely that younger erythrocytes that get damaged due to oxidative or other forms of stress may readily extrude PS and undergo erythrophagocytosis, leading to random killing of erythrocytes. On the other hand, a steady fall in CD47 [14] and CD147 [11] expression has been observed during aging of erythrocytes (**Figure 2C** and **D**). These may render older erythrocytes susceptible to phagocytosis by macrophages.

4. Murine models of anemia

4.1. Cadmium (Cd)-induced anemia

Cadmium, one of the most toxic heavy metals, a category I carcinogen [21], is a nonbiodegradable environmental contaminant that can cause serious health hazard [21–24]. Exposure to cadmium may occur through contamination in food and drinking water [25], cigarette smoke [26, 27], or through occupational exposure in mining and manufacturing industries [23, 27, 28]. Cadmium has a long biological half-life of 10–30 years and can accumulate into various organs and tissues, particularly in kidneys [29] and also in the lung, liver, bone, testis, cardiovascular, and the immune systems, causing severe damage [29, 30]. Anemia as a consequence of cadmium toxicity has been observed in many cases of human exposure [31–33] and also in animal models [34–38].

In our experiment groups of mice were given 1000 ppm of cadmium chloride in drinking water, and their blood parameters were monitored every week. Continuous exposure to cadmium induced a significant decline in erythrocyte count and hemoglobin content, indicating anemia (**Figure 3**, panels A and B). A significant decline in blood parameters could be observed as early as in the second week of exposure [17]. Exposure to lower dose of cadmium (50 ppm $CdCl_2$) resulted in the development of a transient anemia in mice [17].

4.2. Herbicide Paraquat (PQ)-induced anemia

Paraquat (N, N′-dimethyl-4, 4′-bipyridinium dichloride, PQ), one of the most widely used herbicide, kills plants rapidly by deactivating the photosynthetic mechanism. It also has considerable toxicity toward animals and humans and has widely been used for suicide throughout the world [39–41]. Ingestion of PQ causes liver, lung, heart, and kidney failure within several

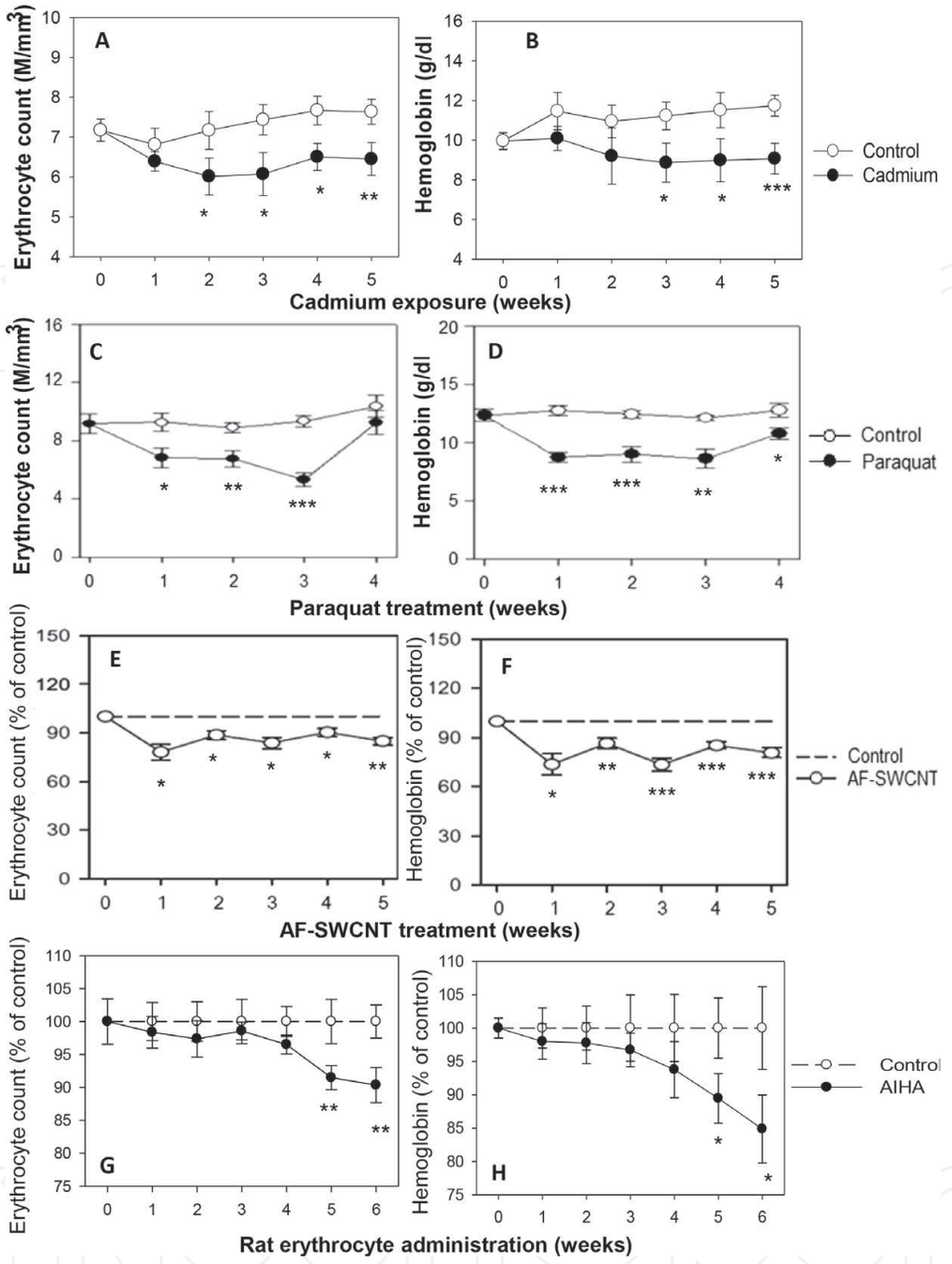

Figure 3. Induction of anemia in mice. Anemia was induced in mice through different stimuli. Blood samples from mice were collected at different time points and analyzed on an automated cell counter. Erythrocyte count and hemoglobin content in cadmium (Cd)-induced anemia (panels A and B), Paraquat (PQ)-induced anemia (panels C and D), carbon nanotube (CNT)-induced anemia (panels E and F), and autoimmune hemolytic anemia (AIHA, panels G and H) are shown above. Each point on the graph represents mean ±SEM of observations. n = 10. *$p < 0.05$, **$p < 0.01$, and ****$p < 0.001$ for comparison of the groups. Statistical analysis was done using Student t-test.

days to several weeks [42]. A link between the exposure to PQ and Parkinson's disease has also been reported [43]. PQ is a potent inducer of reactive oxygen species (ROS), and occurrence of anemia as a consequence of exposure to PQ has also been documented [44, 45]. The use of PQ was banned in Europe in 2007, but the herbicide is still widely used in the rest of the world.

In our experiment mice were administered repeated doses of Paraquat (Paraquat dichloride hydrate freshly dissolved in phosphate buffered saline (PBS), 10 mg/kg of body weight) intraperitoneally (*i.p.*) on alternate days [18, 43]. Control mice received vehicle alone. Blood parameters were monitored at different time points. Paraquat treatment induced a transient anemia in mice, indicated by a significant decline in blood erythrocyte count (up to 45%) as well as blood hemoglobin levels (upto 38%) on 7, 14, and 21 day time points (**Figure 3**, panels C and D) [18]. Erythrocyte count as well as blood hemoglobin levels however returned to normal by the end of 4 weeks, even though PQ treatment was continued.

4.3. Carbon nanotube (CNT)-induced anemia

Nanoparticles are defined as particulate dispersions or solid particles with a size in the range of 10–100 nm. Single-walled carbon nanotubes (SWCNTs) are a class of engineered nanomaterials that represent rolled-up tubes of graphite sheet of sp2 hybridized carbon atoms, having a diameter of about 1 nm. Due to their unique structural and remarkable electronic, mechanical, and chemical properties, engineered nanomaterials find wide applications in molecular electronics, microdevices, gas storage, catalytic supports, aerospace, automobile, and atomic force microscopy and biological applications like biosensors, drug delivery, etc. [46–48]. Interaction of nanoparticles with the body is dependent on their size, chemical composition, surface structure, solubility, and shape [49–51]. Several studies have demonstrated the toxicity of SWCNT to different types of cells *in vitro* [52–54] and *in vivo* [55–58].

In our experiment, mice were administrated *i.v.* 10 mg acid-functionalized SWCNTs (AF-SWCNTs) on alternate days, and blood parameters were examined at different time points. Significant decline in erythrocyte count as well as hemoglobin levels was observed at different time points during the treatment with AF-SWCNTs [19]. Results in **Figure 3**, panels E and F show that erythrocyte count and hemoglobin levels decreased by 10–22% and 13–25%, respectively, at different time points. Repeated administration of AF-SWCNTs (10 mg) induced a sustained anemia in mice [19].

4.4. Autoimmune hemolytic anemia (AIHA)

Autoimmune hemolytic anemia (AIHA) is characterized by the production of pathogenic self-reactive autoantibodies against self-erythrocytes that can result in premature destruction of erythrocytes leading to the clinical manifestation of anemia [59–62]. Pathogenesis of AIHA involves two underlying mechanisms, namely erythrophagocytosis of autoantibody-coated erythrocytes by macrophages in the reticuloendothelial system in the liver and spleen [63, 64] and complement-mediated lysis of erythrocytes following binding of IgM autoantibodies [65].

AIHA could be induced in mice following the Playfair and Clarke Model [66], based on Weigle's hypothesis of termination of immunological unresponsiveness to an antigen by injection of a cross-reacting antigen with similar/shared epitopes [67]. In this model repeated injection of rat erythrocytes induces production of autoantibodies against self-erythrocytes in mice [68–70]. The immunized mice develop autoimmune anemia, a severe but transient one, characterized by the presence of both anti-mouse autoantibody and the usual anti-rat antibody [69].

In our experiment mice were given weekly *i.p.* injections of 2×10^8 rat erythrocytes, and blood parameters were monitored at regular intervals. Generation of anti-mouse erythrocyte autoantibody was estimated by flow cytometric analysis of erythrocytes stained with anti-mouse IgG/IgM-fluorescein isothiocyanate (FITC) polyclonal antibodies [71, 72]. The results show that a significant anemia was demonstrable in the immunized mice only after 5–6 weekly administrations of rat erythrocytes [20], when the blood erythrocyte count suffered a 10% decline and hemoglobin a staggering 15% decline (**Figure 3**, panels G and H, respectively). The anti-mouse erythrocyte autoantibody level also showed a sharp increase at the same time point [20], indicating an autoimmune response.

5. Erythrocyte turnover pattern in different models of anemia

Turnover profile for the various age cohorts of circulating erythrocytes was examined by utilizing the DIB technique of erythrocyte labeling *in vivo* to analyze the age-dependent susceptibility of circulating erythrocytes to the different mediators of stress, Cd, PQ, CNTs, and AIHA. Erythrocytes isolated from the peripheral blood of the DIB-labeled mice were stained *ex vivo* with streptavidin-allophycocyanin (APC) and anti-mouse CD71-PE followed by flow cytometry. Circulating erythrocytes were delineated as per the relative streptavidin and CD71 staining into four different groups: biotin^{high} (older erythrocytes), biotin^{low} (intermediate age group), CD71$^-$biotin^{negative} (young) erythrocytes, and CD71$^+$biotin^{negative} reticulocytes. A representative flow diagram is shown in **Figure 4**. A comparison of the proportion of erythrocytes

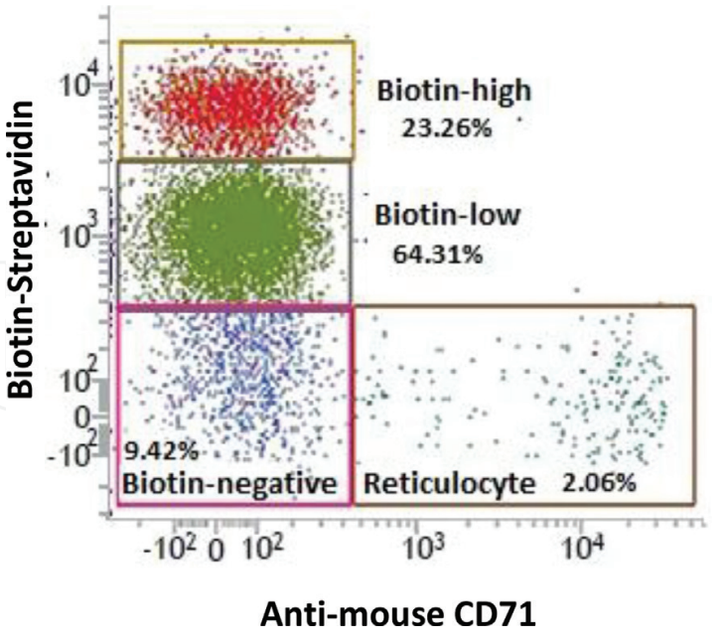

Figure 4. Age cohorts of circulating erythrocytes. Mouse erythrocytes were labeled with biotin *in vivo* by the two-step biotinylation procedure (DIB protocol B). Blood samples were collected, and erythrocytes were stained *ex vivo* with streptavidin-APC and anti-mouse CD71-PE. Proportions of the different age cohorts were determined as biotin^{high} (older erythrocytes), biotin^{low} (intermediate age group), CD71$^-$biotin^{negative} (young erythrocytes), and CD71$^+$biotin^{negative} reticulocytes. Representative flow histograms showing the proportion of different age groups of erythrocytes are shown.

belonging to different age cohorts would give their turnover profile. Interestingly, results from the four models of murine anemia could be clustered into two distinct categories, with completely contrasting characters.

5.1. Increased susceptibility of older erythrocytes: Cd and PQ

Exposure to environmental toxicants cadmium and Paraquat resulted in a very similar response in terms of erythrocyte turnover. The turnover profiles indicate that the kinetics of decline of older erythrocytes (biotin^{high} subpopulations that entered blood circulation before the first biotinylation step; **Figure 5**, panels A and B) and the increase in the proportion of younger subpopulation of erythrocytes (biotin^{negative}, entering blood circulation after the second biotinylation step; **Figure 5**, panels C and D) was significantly higher in the treatment groups than the control (**Figure 5**) [17, 18]. These results suggest that the older erythrocytes in blood circulation may be preferentially eliminated in the toxicant (Cd or PQ)-exposed mice, leaving the young

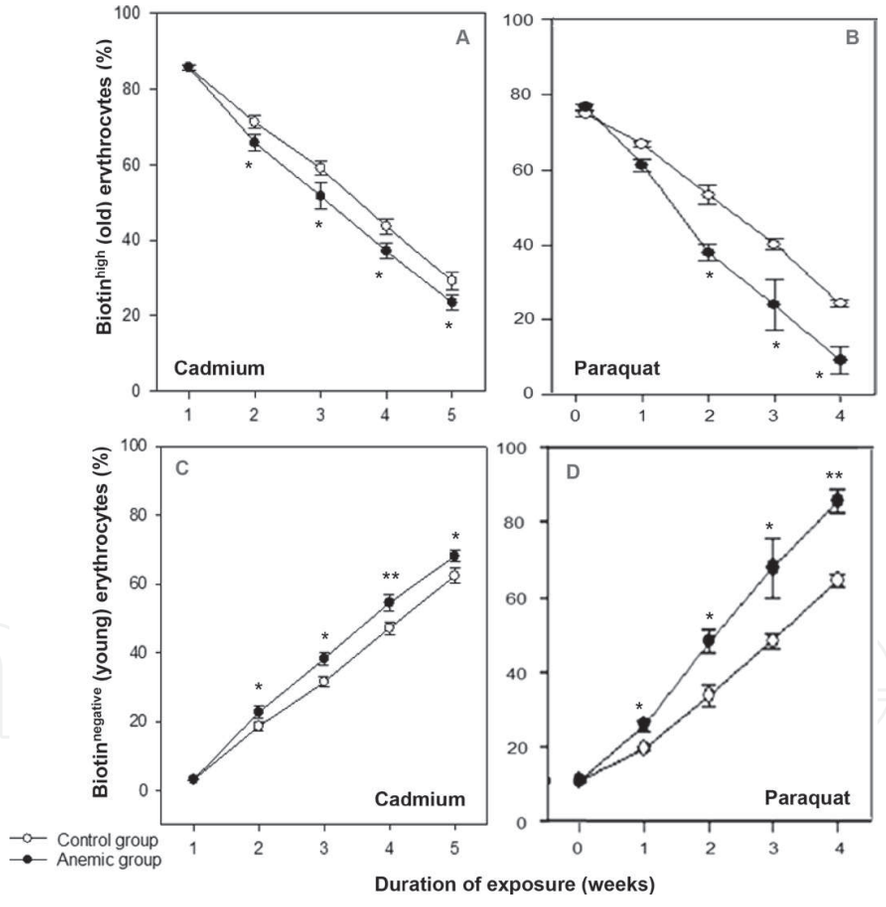

Figure 5. Erythrocyte turnover in the blood of mice exposed to cadmium and Paraquat. Mice were rendered anemic by exposure to toxicants like cadmium and Paraquat. Mouse erythrocytes were labeled with biotin *in vivo* by the two-step biotinylation procedure (protocol A). Erythrocytes were stained *ex vivo* with streptavidin-APC, and proportions of the different age cohorts were determined. Turnover profile of relatively aged biotin^{high} (panels A and B) and young biotin^{negative} (panels C and D) erythrocytes in cadmium-treated (panels A and C) and Paraquat-treated (panels B and D) mice has been shown above. Each point on the graph represents mean ±SEM of observations. n = 10. *$p < 0.05$ and **$p < 0.01$ for comparison of the groups. Statistical analysis was done using Student t-test.

erythrocytes to accumulate in circulation, indicated by the significant increase in the proportion of the younger biotin^{negative} erythrocytes. This could indicate either an increased generation of fresh erythrocytes or prolonged life span of younger erythrocytes in blood circulation.

The latter view is again supported by the enhanced reticulocytosis in both cadmium-induced and Paraquat-induced anemia (**Figure 6**). An initial surge of reticulocytes in mice exposed to cadmium and Paraquat was clearly seen. This surge was however lost by the fourth and fifth weeks of cadmium (**Figure 6A**) [17] and Paraquat (**Figure 6B**) [18] exposure, respectively.

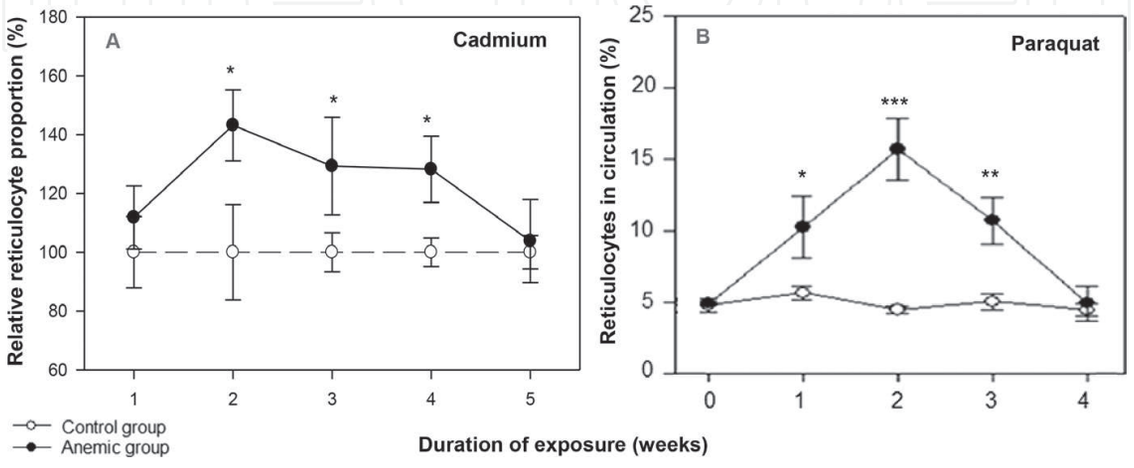

Figure 6. Circulating reticulocytes in cadmium- and Paraquat-induced anemia. Mice were rendered anemic by exposure to toxicants like cadmium chloride and Paraquat. Blood was collected at regular interval, and mouse erythrocytes were stained *ex vivo* with anti-mouse CD71-PE to determine the proportion of circulating reticulocytes through flow cytometry. Panel A shows the relative proportions of reticulocytes in cadmium-fed mice. For this, the mean reticulocyte counts in control mice at each time point was taken as 100, and the proportion of reticulocytes in the exposed groups was estimated in relative terms. Panel B shows the reticulocyte proportion in the Paraquat-treated mice. Each point on the graph represents mean ±SEM of observations. n = 10. *$p < 0.05$, **$p < 0.01$, and ***$p < 0.005$ for comparison of the groups. Statistical analysis was done using Student t-test.

5.2. Increased susceptibility of young erythrocytes: CNTs and AIHA

Autoimmune hemolytic anemia (AIHA) and anemia induced by exposure to AF-SWCNTs are characterized by a unique turnover profile of circulating erythrocytes, which is radically different from the one observed in Cd- and PQ-induced anemia. There is a significant increase (twofold) in the proportion of older erythrocyte population (biotin^{high}, **Figure 7**, panels A and C) along with a concomitant decline in the proportion of young erythrocytes (**Figure 7**, panels B and D). Thus relatively younger erythrocytes in the blood seem to be preferentially eliminated in conditions of AIHA- [20] and CNT-induced anemia [19] either by macrophage-mediated erythrophagocytosis in the reticuloendothelial system of the spleen or by complement-mediated lysis.

In the turnover profile though comparable in both AIHA- and CNT-induced anemia, the two models revealed very different results in terms of the reticulocyte response. The AF-SWCNT treatment resulted in reticulocytosis, showing > twofold increase in the percentage of blood reticulocytes from 2.23 to 5.32% (**Figure 8A**) [19]. Autoimmune anemia on the other hand resulted in severe reticulocytopenia, showing a 16–18% decline in reticulocyte proportion as seen in **Figure 8**, panel B [20].

http://dx.doi.org/10.5772/intechopen.69133

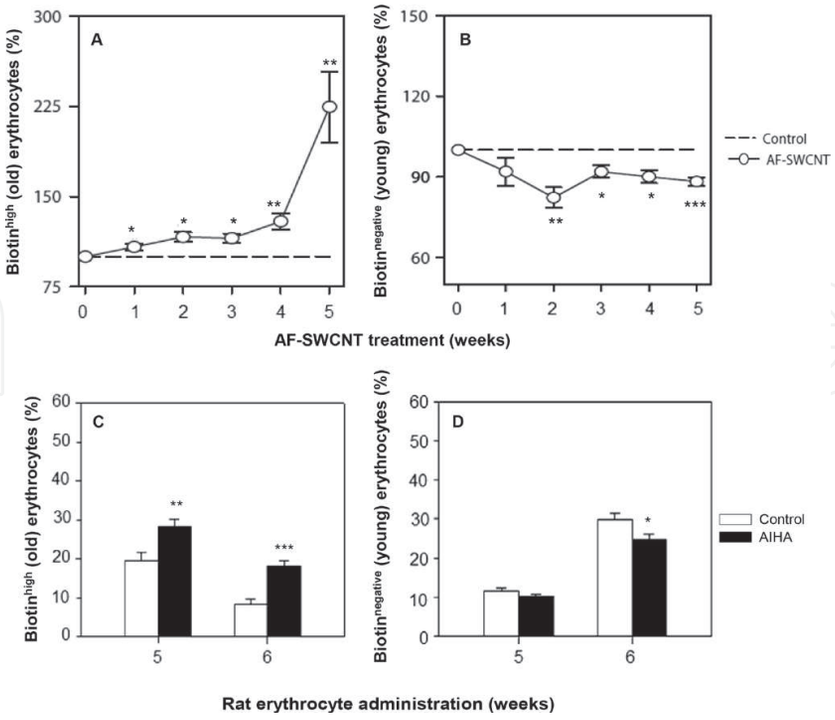

Figure 7. Erythrocyte turnover in the blood of AIHA mice and mice exposed to AF-SWCNTs. Mice were rendered anemic by injecting AF-SWCNTs or by inducing AIHA. Mouse erythrocytes were labeled with biotin *in vivo* by the two-step biotinylation procedure (protocol A for CNT-induced anemia; protocol B for AIHA). Erythrocytes were stained *ex vivo* with streptavidin-APC, and proportions of the different age cohorts were determined. Turnover profile of relatively aged biotin^{high} (panels A and C) and young biotin^{negative} (panels B and D) erythrocytes in AF-SWCNT-treated mice (panels A and B) and AIHA mice (panels C and D) has been shown above. The time point for AIHA has been selected on the basis of the induction of anemia (only after the fifth and sixth immunization doses). Each point and each bar on the graph represent mean ±SEM of observations. n = 10. *$p < 0.05$, **$p < 0.01$, and ***$p < 0.005$ for comparison of the groups. Statistical analysis was done using Student t-test.

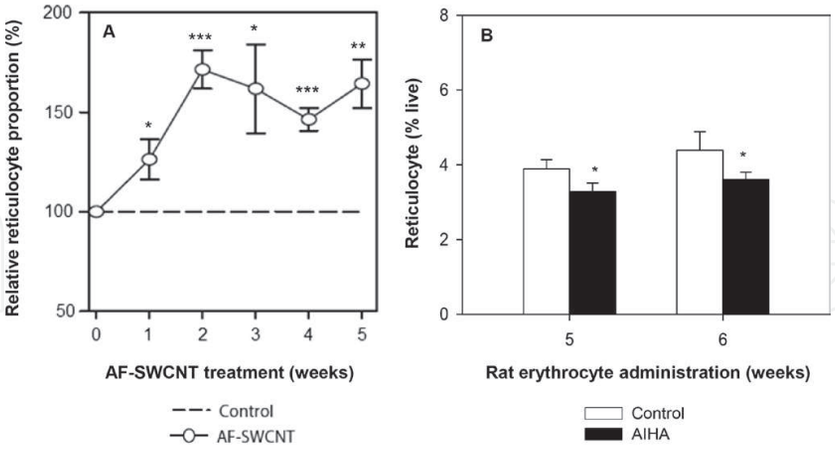

Figure 8. Circulating reticulocytes in the blood of AIHA mice and mice exposed to AF-SWCNTs. Mice were rendered anemic by injecting AF-SWCNTs or by inducing AIHA. Blood was collected at regular interval, and mouse erythrocytes were stained *ex vivo* with anti-mouse CD71-PE to determine the proportion of circulating reticulocytes through flow cytometry. Panel A shows the relative proportions of reticulocytes in AF-SWCNT-treated mice. For this, the mean reticulocyte counts in control mice at each time point was taken as 100, and the proportion of reticulocytes in the exposed groups was estimated in relative terms. Panel B shows the reticulocyte proportion in the AIHA mice. The time point for AIHA has been selected on the basis of the induction of anemia (only after the fifth and sixth immunization doses). Each point and each bar on the graph represent mean ±SEM of observations. n = 10. *$p < 0.05$, **$p < 0.01$, and ***$p < 0.005$ for comparison of the groups. Statistical analysis was done using Student t-test.

6. Conclusion

The technique of double *in vivo* biotinylation has been used extensively in our laboratory to unravel the changes associated with erythrocyte aging in circulation. In the present study, the same DIB technique has been used to track the stress-related changes in different age cohorts of erythrocytes and ascertain their susceptibility in different types of anemia. To achieve this goal, we have compared the erythrocyte turnover patterns in four different models of murine anemia, namely anemia induced by (a) toxic heavy metal cadmium (Cd) ions, (b) herbicide Paraquat (PQ), (c) carbon nanotubes (CNTs), and (d) autoantibody in autoimmune hemolytic anemia (AIHA). Interestingly, the study revealed two distinct and contrasting patterns of erythrocyte turnover in murine anemia. This difference could be because of the difference in the way the stress inducers interact with the cell in each of the models. In certain types of anemia, where erythrocytes are exposed to toxicants that directly enter the cells, like in the case of cadmium [73] and Paraquat [74, 75], the stress inducers might interfere with enzyme activities and signaling processes, thereby promoting senescent changes within the cell. Therefore in toxicant stress, as in cadmium-induced anemia and Paraquat-induced anemia, older erythrocytes that are already undergoing senescent changes become more susceptible and are preferentially removed from circulation [17, 18]. On the other hand, in some other cases, where erythrocytes are exposed to agents that directly interact with the cell membrane, as in the case of AIHA- [70, 76] and AF-SWCNT-induced anemia [57], younger erythrocytes in blood circulation are preferentially removed [19, 20]. This biasness could be due to the difference in the membrane composition in the different age cohorts of erythrocytes [77–79]. The fate of the erythrocytes in anemic mice therefore depends on the characteristics and behavior of the stress mediator and therefore may be different in different types of anemia.

Acknowledgements

The work was funded by three research grants from the Department of Science and Technology (DST), Government of India, to RKS. SC received Senior Research Fellowship from Council of Scientific and Industrial Research (CSIR), New Delhi. Figures used in this manuscript have been compiled from various research publications [11, 12, 14–20].

Appendices and nomenclatures

AF-SWCNT	Acid-functionalized single-walled carbon nanotube
AIHA	Autoimmune hemolytic anemia
ANOVA	Analysis of variance
APC	Allophycocyanin

BXN	Biotin-X-N-hydroxysuccinimide ester
CD	Cluster of differentiation
Cd	Cadmium
$CdCl_2$	Cadmium chloride
CNT	Carbon nanotubes
DIB	Double *in vivo* biotinylation
FITC	Fluorescein isothiocyanate
Ig	Immunoglobulin
i.p.	Intraperitoneal
i.v.	Intravenous
NHS	N-hydroxysuccinimide
PBS	Phosphate-buffered saline
PE	Phycoerythrin
ppm	Parts per million
PQ	Paraquat
PS	Phosphatidylserine
RES	Reticuloendothelial system
ROS	Reactive oxygen species
SEM	Standard error of the mean
SWCNT	Single-walled carbon nanotube

Author details

Sreoshi Chatterjee and Rajiv K. Saxena*

*Address all correspondence to: rajivksaxena@hotmail.com

Faculty of Life Sciences and Biotechnology, South Asian University, New Delhi, India

References

[1] Goodman JW, Smith LH. Erythrocyte life span in normal mice and in radiation bone marrow chimeras. American Journal of Physiology. 1961;**200**:764-770

[2] Horky J, Vacha J, Znojil V. Comparison of life span of erythrocytes in some inbred strains of mouse using 14C-labelled glycine. Physiologia Bohemoslovenica. 1978;**27**:209-217

[3] Piomelli S, Seaman C. Mechanism of red blood cell aging: Relationship of cell density and cell age. American Journal of Hematology. 1993;**42**:46-52

[4] Clark MR. Senescence of red blood cells: Progress and problems. Physiological Reviews. 1988;**68**:503-554

[5] Morrison M, Jackson CW, Mueller TJ, Huang T, Dockter ME, Walker WS, et al. Does cell density correlate with red cell age? Biomedica Biochimica Acta. 1983;**42**:107-111

[6] Clark MR, Shohet SB. Red cell senescence. Clinics in Haematology. 1985;**14**:223-257

[7] Mueller TJ, Jackson CW, Dockter ME, Morrison M. Membrane skeletal alterations during *in vivo* mouse red cell aging. Increase in the band 4.1a:4.1b ratio. Journal of Clinical Investigation. 1987;**79**:492-499

[8] Suzuki T, Dale GL. Biotinylated erythrocytes: *In vivo* survival and *in vitro* recovery. Blood. 1987;**70**:791-795

[9] Suzuki T, Dale GL. Senescent erythrocytes: Isolation of *in vivo* aged cells and their biochemical characteristics. Proceedings of the National Academy of Sciences of the United States of America. 1988;**85**:1647-1651

[10] Hoffmann-Fezer G, Mysliwietz J, Mortlbauer W, Zeitler HJ, Eberle E, Honle U, et al. Biotin labeling as an alternative nonradioactive approach determination of red cell survival. Annals of Hematology. 1993;**67**:81-87

[11] Khandelwal S, Saxena RK. Assessment of survival of aging erythrocyte in circulation and attendant changes in size and CD147 expression by a novel two step biotinylation method. Experimental Gerontology. 2006;**41**:855-861

[12] Khandelwal S, Saxena RK. A role of phosphatidylserine externalization in clearance of erythrocytes exposed to stress but not in eliminating aging populations of erythrocyte in mice. Experimental Gerontology. 2008;**43**:764-770

[13] Khandelwal S, Saxena RK. Age-dependent increase in green autofluorescence of blood erythrocytes. Journal of Biosciences. 2007;**32**:1139-1145

[14] Khandelwal S, van Rooijen N, Saxena RK. Reduced expression of CD47 during murine red blood cell (RBC) senescence and its role in RBC clearance from the circulation. Transfusion. 2007;**47**(9):1725-1732

[15] Saxena RK, Khandelwal S. Aging and destruction of blood erythrocytes in mice. Current Science. 2009;**97**(4):500-507

[16] Saxena RK, Bhardwaj N, Sachar S, Puri N, Khandelwal S. A Double *in vivo* biotinylation (DIB) technique for objective assessment of aging and clearance of mouse erythrocytes in blood circulation. Transfusion Medicine and Hemotherapy. 2012;**39**:335-341

[17] Chatterjee S, Saxena RK. Preferential elimination of older erythrocytes in circulation and depressed bone marrow erythropoietic activity to cadmium induced anemia in mice. PLoS One. 2015;**10**(7):e0132697

[18] Bhardwaj N, Saxena RK. Elimination of young erythrocytes from blood circulation and altered erythropoietic patterns during paraquat induced anemic phase in mice. PLoS One. 2014;**9**(6):e99364

[19] Bhardwaj N, Saxena RK. Selective loss of younger erythrocytes from blood circulation and changes in erythropoietic patterns in bone marrow and spleen in mouse anemia induced by poly-dispersed single wall carbon nanotubes. Nanotoxicology. 2015;**9**(8):1032-1040

[20] Chatterjee S, Bhardwaj N, Saxena RK. Identification of stages of erythroid differentiation in bone marrow and erythrocyte subpopulations in blood circulation that are preferentially lost in autoimmune hemolytic anemia in mouse. Plos One. 2016;**11**(11):e0166878

[21] IARC. Cadmium and Cadmium Compounds. IARC Monographs Volume 58. 1993. Available from: http://monographs.iarc.fr/ENG/Monographs/vol58/mono58-7.pdf. [Accessed: 21-20-2017]

[22] WHO. Exposure to Cadmium: A Major Public Health Concern. 2010. Availablefrom: http://www.who.int/ipcs/features/cadmium.pdf?ua=1 [Accessed 2017-02-21]

[23] ATSDR. Toxicological Profile for Cadmium. U.S. Department of Health and Human Services, Public Health Service. 2012. Available from: https://www.atsdr.cdc.gov/toxprofiles/tp5.pdf [Accessed 21-02-2017]

[24] Satarug S, Garrett SH, Sens MA, Sens DA. Cadmium, environmental exposure, and health outcomes. Environmental Health Perspectives. 2010;**118**(2):182-190

[25] Franz E, Römkens P, van Raamsdonk L, van der Fels-Klerx I. A chain modeling approach to estimate the impact of soil cadmium pollution on human dietary exposure. Journal of Food Protection. 2008;**71**(12):2504-2513

[26] Järup L, Berglund M, Elinder CG, Nordberg G, Vahter M. Health effects of cadmium exposure—a review of the literature and a risk estimate. Scandinavian Journal of Work, Environment & Health. 1998;**24**(1):1-51

[27] Satarug S, Moore MR. Adverse health effects of chronic exposure to low-level cadmium in foodstuffs and cigarette smoke. Environmental Health Perspectives. 2004;**112**:1099-1103

[28] Sorahan T, Lister A, Gilthorpe MS, Harrington JM. Mortality of copper cadmium alloy workers with special reference to lung cancer and non-malignant diseases of the respiratory system, 1946-92. Occupational and Environmental Medicine 1995;**52**:804-812

[29] J'arup L, Akesson A. Current status of cadmium as an environmental health problem. Toxicology and Applied Pharmacology. 2009;**238**:201-208

[30] Nawrot TS, Staessen JA, Roels HA, Munters E, Cuypers A, Richart T, et al. Cadmium exposure in the population: From health risks to strategies of prevention. Biometals. 2010;**23**:769-782

[31] Horiguchi H, Teranishi H, Niiya K, Aoshima K, Katoh T, Sakuragawa N, et al. Hypoproduction of erythropoietin contributes to anemia in chronic cadmium intoxication: Clinical study on Itai-itai disease in Japan. Archives of Toxicology. 1994;**68**(10):632-636

[32] Horiguchi H, Aoshima K, Oguma E, Sasaki S, Miyamoto K, Hosoi Y, et al. Latest status of cadmium accumulation and its effects on kidneys, bone, and erythropoiesis in inhabitants of the formerly cadmium-polluted Jinzu River basin in Toyama, Japan after restoration of rice paddies. International Archives of Occupational and Environmental Health. 2010;**83**:953-970

[33] Gluhcheva Y, Ivanov I, Atanasov V, Antonova N, Ivanovad Ju, Mitewa M. Hematological changes in case of chronic cadmium intoxication and monensin detoxication. Relationship with rheological variables. Clinical Hemorheology and Microcirculation. 2011;**49**:417-422

[34] Jacobs RM, Fox MRS, Aldridge MH. Changes in Plasma Proteins Associated with the Anemia Produced by Dietary Cadmium in Japanese quail. Journal of Nutrition. 1969;**99**: 119-128

[35] Pond WG, Walker EF Jr., Kirtland D. Cadmium-induced anemia in growing pigs: Protective effect of oral or parenteral iron. Journal of Animal Science 1973;**36**:1122-1124

[36] Sakata S, Iwami K, Enoki Y, Kohzuki H, Shimizu S, Matsuda M, et al. Effects of cadmium on *in vitro* and *in vivo* erythropoiesis: Erythroid progenitor cells (CFU-E), iron, and erythropoietin in cadmium-induced iron deficiency anemia. Experimental Hematology. 1988;**16**:581-587

[37] Horiguchi H, Oguma E, Kayama F. Cadmium and cisplatin damage erythropoietin-producing proximal renal tubular cells. Archives of Toxicology. 2006;**80**:680-686

[38] Horiguchi H, Oguma E, Kayama F. Cadmium Induces Anemia through Interdependent Progress of Hemolysis, Body Iron Accumulation, and Insufficient Erythropoietin Production in Rats. Toxicological Sciences. 2011;**122**(1):198-210

[39] Bismuth C, Garnier R, Baud FJ, Muszynski J, Keyes C. Paraquat poisoning. An overview of the current status. Drug Safety. 1990;**5**:243-251

[40] Dawson AH, Eddleston M, Senarathna L, Mohamed F, Gawarammana I, Bowe SJ, et al. Acute human lethal toxicity of agricultural pesticides: A prospective cohort study. PLoS Medicine 2010;**7**:e1000357

[41] Eddleston M. Patterns and problems of deliberate self-poisoning in the developing world. QJM 2000;**93**:715-731

[42] Bullivant CM. Accidental poisoning by paraquat: Report of two cases in man. British Medical Journal 1966;**1**:1272-1273

[43] Prasad K, Tarasewicz E, Mathew J, Strickland PA, Buckley B, et al. Toxicokinetics and toxicodynamics of paraquat accumulation in mouse brain. Experimental Neurology. 2009;**215**:358-367

[44] Joenje H, Nieuwint AW, Oostra AB, Arwert F, de Koning H, et al. Cytogenetic toxicity of paraquat and streptonigrin in Fanconi's anemia. Cancer Genetics and Cytogenetics. 1987;**25**:37-45

[45] Prihartono N, Kriebel D, Woskie S, Thetkhathuek A, Sripaung N, et al. Risk of aplastic anemia and pesticide and other chemical exposures. Asia-Pacific Journal of Public Health. 2011;**23**:369-377

[46] Baughman RH, Zakhidov AA, de Heer WA. Carbon nanotubes—the route toward applications. Science. 2002;**297**:787-792

[47] Bianco A, Kostarelos K, Prato M. Applications of carbon nanotubes in drug delivery. Current Opinion in Chemical Biology. 2005;**9**:674-679

[48] Kam NW, O'Connell M, Wisdom JA, Dai H. Carbon nanotubes as multifunctional biological transporters and near-infrared agents for selective cancer cell destruction. Proceedings of the National Academy of Sciences of the United States of America. 2005;**102**:11600-11605

[49] Chithrani BD, Ghazani AA, Chan WC. Determining the size and shape dependence of gold nanoparticle uptake into mammalian cells. Nano Letters. 2006;**6**:662-668

[50] Jiang J, Oberdorster G, Elder A, Gelein R, Mercer P, Biswas P. Does nanoparticle activity depend upon size and crystal phase? Nanotoxicology. 2008;**2**:33-42

[51] Sohaebuddin SK, Thevenot PT, Baker D, Eaton JW, Tang L. Nanomaterial cytotoxicity is composition, size, and cell type dependent. Particle and Fibre Toxicology. 2010;**7**:22-39

[52] Davoren M, Herzog E, Casey A, Cottineau B, Chambers G, Byrne HJ, Lyng FM. *In vitro* toxicity evaluation of single walled carbon nanotubes on human A549 lung cells. Toxicology *In Vitro*. 2007;**21**:438-448

[53] Saxena RK, Williams W, Mcgee JK, Daniels MJ, Boykin E, Gilmour MI. Enhanced *in vitro* and *in vivo* toxicity of poly-dispersed acid-functionalized single-wall carbon nanotubes. Nanotoxicology. 2007;**1**(4):291-300

[54] Kumari M, Sachar S, Saxena RK. Loss of proliferation and antigen presentation activity following internalization of polydispersed carbon nanotubes by primary lung epithelial cells. PLoS One. 2012;**7**:e31890

[55] Lam CW, James JT, McCluskey R, Hunter RL. Pulmonary toxicity of single-wall carbon nanotubes in mice 7 and 90 days after intratracheal instillation. Toxicological Sciences 2004;**77**:126-134

[56] Tong H, McGee JK, Saxena RK, Kodavanti UP, Devlin RB, Gilmour MI. Influence of acid functionalization on the cardiopulmonary toxicity of carbon nanotubes and carbon black particles in mice. Toxicology and Applied Pharmacology. 2009;**239**:224-232

[57] Sachar S, Saxena RK. Cytotoxic effect of poly-dispersed single walled carbon nanotubes on erythrocytes *in vitro* and *in vivo*. PLoS One. 2011;**6**(7):e22032

[58] Alam A, Sachar S, Puri N, Saxena RK. Interactions of polydispersed single-walled carbon nanotubes with T cells resulting in downregulation of allogeneic CTL responses *in vitro* and *in vivo*. Nanotoxicology. 2013;**7**:1351-1360

[59] Sokol RJ, Hewitt S. Autoimmune hemolysis: A critical review. Critical Reviews in Oncology/Hematology. 1985;**4**:125-154

[60] Sokol RJ, Booker DJ, Stamps R. The pathology of autoimmune haemolytic Anaemia. Journal of Clinical Pathology. 1992;**45**:1047-1052

[61] Hashimoto C. Autoimmune hemolytic anemia. Clinical Reviews in Allergy & Immunology. 1998;**16**(3):285-295

[62] Gehrs BC, Friedberg RC. Autoimmune hemolytic anemia. American Journal of Hematology. 2002;**69**:258-271

[63] Engelfriet CP, Overbeeke MA, von dem Borne AE. Autoimmune hemolytic anemia. Seminars in Hematology. 1992;**29**:3-12

[64] Izui S, Berney T, Shibata T, Fulpius T, Fossati L, Merino R. Molecular and cellular basis for pathogenicity of autoantibodies. Tohoku Journal of Experimental Medicine 1994;**173**: 15-30

[65] Jefferies LC. Transfusion therapy in autoimmune hemolytic anemia. Hematology/ Oncology Clinics of North America 1994;**8**:1087-1104

[66] Playfair JHL, Marshall-Clarke S. Induction of red cell autoantibodies in normal mice. Nature: New Biology. 1973;**243**:213-214

[67] Weigle WO. Recent observations and concepts in immunological unresponsiveness and autoimmunity. Clinical and Experimental Immunology. 1971;**9**:437-447

[68] Cox KO, Keast D. Erythrocyte autoantibodies induced in mice immunized with rat erythrocytes. Immunology. 1973;**25**:531-539

[69] Naysmith JD, Ortega-Pierres MG, Elson CJ. Rat erythrocyte induced anti-erythrocyte autoantibody production and control in normal mice. Immunology Reviews 1981;**55**: 55-87

[70] Barker RN, Casswell KM, Elson CJ. Identification of murine erythrocyte autoantigens and cross-reactive rat antigens. Immunology. 1993;**78**:568-573

[71] Arndt PA, Garratty G. Flow cytometric analysis in red blood cell immunology. Transfusion Medicine and Hemotherapy. 2004;**31**:163-174

[72] Thedsawad A, Taka A, Wanachiwanawin W. Development of flow cytometry for detection and quantitation of red cell bound immunoglobulin G in autoimmune hemolytic anemia with negative direct Coombs test. Asian Pacific Journal of Allergy and Immunology. 2011;**29**:364-367

[73] Nordberg GF, Kjellstrom T, Nordberg G. Kinetics and metabolism. In: Friberg L, Elinder CG, Kjellstrom T, Nordberg GF, editors. Cadmium and health: A toxicological and epidemiological appraisal. Boca Raton: CRC Press; 1986. pp. 103-178

[74] Chen N, Bowles MR, Pond SM. Prevention of paraquat toxicity in suspensions of alveolar type II cells by paraquat-specific antibodies. Human & Experimental Toxicology. 1994;**13**:551-557

[75] Grabie V, Scemama JL, Robertson JB, Seidel ER. Paraquat uptake in the cultured gastrointestinal epithelial cell line, IEC-6. Toxicology and Applied Pharmacology. 1993;**122**:95-100

[76] Barker RN, Shen C-R, Elson CJ. T-cell specificity in murine autoimmune haemolytic anaemia induced by rat red blood cells. Clinical and Experimental Immunology. 2002;**129**:208-213

[77] Bosman GJCGM, Were JM, Willekens FLA, Novotny VMJ. Erythrocyte ageing *in vivo* and *in vitro*: Structural aspects and implications for transfusion. Transfusion Medicine 2008;**18**:335-347

[78] Bosman GJCGM. Survival of red blood cells after transfusion: Processes and consequences. Frontiers in Physiology. 2013;**4**:376

[79] Lutz HU, Bogdanova A. Mechanisms tagging senescent red blood cells for clearance in healthy humans. Frontiers in Physiology. 2013;**4**:387

IntechOpen